

Parametric study on earthquake induced pounding between adjacent buildings

Sadegh Naserkhaki*¹, Farah N.A. Abdul Aziz¹ and Hassan Pourmohammad²

¹Department of Civil Engineering, Faculty of Engineering, Universiti Putra Malaysia, Serdang, Malaysia

²Department of Civil Engineering, Faculty of Engineering, Islamic Azad University, Karaj Branch, Karaj, Iran

(Received February 28, 2011, Revised May 22, 2012, Accepted August 7, 2012)

Abstract. Pounding between closely located adjacent buildings is a serious issue of dense cities in the earthquake prone areas. Seismic responses of adjacent buildings subjected to earthquake induced pounding are numerically studied in this paper. The adjacent buildings are modeled as the lumped mass shear buildings subjected to earthquake acceleration and the pounding forces are modeled as the Kelvin contact force model. The Kelvin model is activated when the separation gap is closed and the buildings pound together. Characteristics of the Kelvin model are extensively explored and a new procedure is proposed to determine its stiffness. The developed model is solved numerically and a SDOF pounding case as well as a MDOF pounding case of multistory adjacent buildings are elaborated and discussed. Effects of different separation gaps, building heights and earthquake excitations on the seismic responses of adjacent buildings are obtained. Results show that the seismic responses of adjacent buildings are affected negatively by the pounding. More stories pound together and pounding is more intense if the separation gap is smaller. When the height of buildings differs significantly, the taller building is almost unaffected while the shorter building is affected detrimentally. Finally, the buildings should be analyzed case by case considering the potential earthquake excitation in the area.

Keywords: adjacent buildings; seismic response; Kelvin model; separation gap; pounding; earthquake

1. Introduction

Pounding between adjacent buildings is not avoidable when they vibrate out of phase and the separation gap is not enough to accommodate their relative motions. The pounding which has caused building damage during almost every earthquake (Chopra 2007) is still an issue of the closely located adjacent buildings in dense cities in the earthquake prone areas. This issue has been subject of many researches and got significant progress especially since past two decades.

Generally, the researchers like to model the buildings experimentally and/or numerically. The experimental works cost money and time and are not always accessible so they are limited. Rezavandi and Moghadam (2007), Chau *et al.* (2003), Filiatrault *et al.* (1995), Papadrakakis and Mouzakis (1995) conducted several laboratory tests on the pounding problem and attempted to either develop new numerical methods or validate available numerical methods by means of the acquired results. Although the numerical methods are not as reliable as experimental methods, they

*Corresponding author, Research Assistant, E-mail: snkhaki@gmail.com

reasonably approximate the seismic responses of the pounded adjacent buildings with acceptable accuracy. They are low cost, fast, and flexible that can be extended arbitrarily to consider any desired condition with little efforts, hence feasible.

The first numerical study of the pounding between the adjacent structures during an earthquake was reported in 1976, according to the Wolf and Skrikerud (1980). In the mentioned study, Mahin *et al.* (1976) had simulated the pounding which was occurred at the Olive View Hospital during the San Fernando earthquake. Other well-known pioneers in the building pounding analysis are Davis (1992), Maison and Kasai (1992), Anagnostopoulos and Spiliopoulos (1992), Maison and Kasai (1990), Anagnostopoulos (1988). They developed formulation of the building pounding problem and carried out comprehensive numerical studies in this area. Parameters affecting the building pounding such as building stiffness, building mass, separation gap and different types of contact element were extensively investigated in these studies. Furthermore, the pounding between the adjacent buildings have been concern of many researchers in recent years (Cole *et al.* 2011, Polycarpou and Komodromos 2011, Mahmoud and Jankowski 2010, Favvata *et al.* 2009, Jankowski 2008, Abdel Raheem 2006, Chau and Wei 2001, Pantelides and Mat 1998). In these recent studies, different perspectives of the subject have been considered and improved. Review of these studies reveals a surprising conclusion; not only the results are not consistent to each other but also some of them are contrary because the considered parameters are different. This is why almost all authors believe that the pounding is case dependent and each case must be evaluated individually.

Most of the previous studies have used the contact force element to simulate the pounding forces. One of the most reliable and practical contact force elements is the Kelvin model which is used in this study. Characteristics of the Kelvin model (particularly its stiffness) have not really paid attention because the researchers believed that it does not significantly affect the seismic responses of adjacent buildings. However, it is important that the pounding stiffness do have a very significant effect on produced accelerations which is the major source of damage during the building pounding. Besides, the pounding stiffness governs the pounding duration which has not been precisely explained in the previous studies.

For a nonlinear contact force model a formula has been proposed to determine the pounding stiffness (Muthukumar and DesRoches 2006, Goldsmith 1960). However, there is not a specific formula or method to determine the pounding stiffness for a linear contact force model (e.g., the Kelvin model). The pounding stiffness of linear contact force model has been correlated to the axial stiffness of pounded stories which implies the axially action of the pounding force (Muthukumar and DesRoches 2006, Ruangrassamee and Kawashima 2003, Zhu *et al.* 2002, Maison and Kasai 1990, Anagnostopolus 1988). This is while it has been proved that the pounding induced stresses and displacements are influential in the vicinity of the area of impact with strongly attenuation with distance (Wolf and Skrikerud 1980). Thus the effect of pounding is local and the pounded stories do not experience a perfect axial deformation during instantaneous action of the pounding. Besides, the pounding force follows the rules of impulsive force so the excited elements are not expected to response to the pounding forces during instantaneous pounding.

A numerical procedure to find the pounding stiffness is proposed by Kim and Hon (2003). They show that the pounding magnitude is converged with increment of the pounding stiffness (convergence is occurred when two subsequent pounding magnitudes are equal). The pounding stiffness at the converged state gives the actual pounding stiffness. Their theory is somehow acceptable because the displacement is reduced with increment of the pounding stiffness, thus, their multiplication product may converge to a unique value. Though, this pounding stiffness is not

reliable because the pounding force converges in very high magnitudes and is not consistent to reality. Besides, forms of the two subsequent pounding forces in their work are not compatible. Therefore, finding the value of pounding stiffness is still an issue which is to be solved in this paper.

The aim of this paper is to provide a numerical procedure to obtain the pounding stiffness of the Kelvin model and then to elaborate its application via a SDOF pounding case. Then applying the Kelvin model to a multistory adjacent buildings (MDOF pounding case) and discuss the seismic responses of adjacent buildings due to earthquake induced pounding. A parametric study is to be carried out to investigate effects of different separation gaps, building heights and earthquake excitations for a configuration of a steel building adjacent to a reinforced concrete building.

2. Formulation and solution

2.1 Equation of motion of two adjacent buildings during earthquake induced pounding

The adjacent buildings are assumed two dimensional shear buildings with arbitrary height for each story but same story levels to avoid mid column pounding. Each story of any building has its concentrated mass, viscous damper and linear spring; thus, its own displacement and force in the horizontal direction (Fig. 1). The pounding force at each story level is simulated by the Kelvin

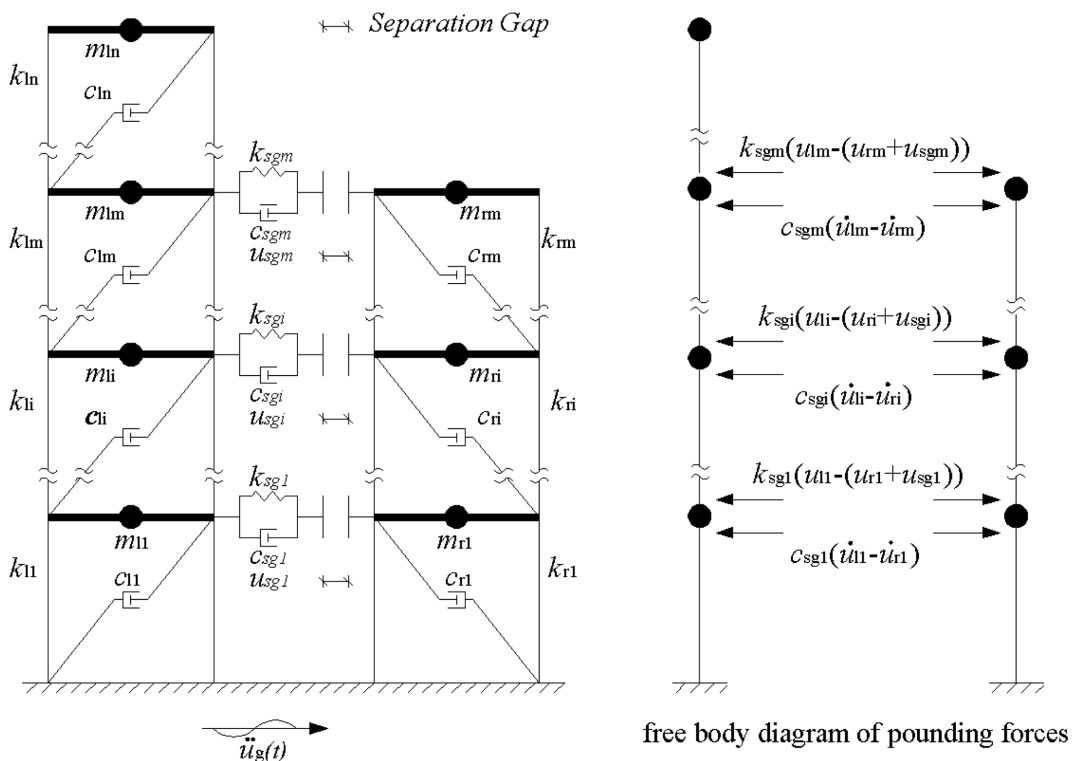


Fig. 1 Lumped mass model of the adjacent buildings connected by the Kelvin model

model that consists of a linear spring to account for pounding induced elastic force and a viscous damper to represent energy dissipation during the pounding (Fig. 1). With these assumptions, equation of motion of two adjacent buildings subjected to earthquake induced pounding is given by

$$\mathbf{m}_b \ddot{\mathbf{u}}_b + \mathbf{c}_b \dot{\mathbf{u}}_b + \mathbf{k}_b \mathbf{u}_b + \mathbf{F} = -\mathbf{m}_b \mathbf{v}_b \ddot{u}_g(t) \tag{1}$$

\mathbf{F} is the vector of pounding forces developed during the pounding between the adjacent buildings. As shown in Fig. 1, pounding force that acts at the pounding instant is equal for pounded adjacent stories but in opposite direction. Now that both pounding induced elastic force and energy dissipation during pounding are taken into account in the Kelvin model, the vector of pounding forces (\mathbf{F}) is correlated to the displacements and velocities of the adjacent buildings as

$$\mathbf{F} = \mathbf{c}_p \dot{\mathbf{u}}_b + \mathbf{k}_p (\mathbf{u}_b - \mathbf{u}_{sg}) \tag{2}$$

Substituting the vector of pounding forces into the Eq. (1) gives

$$\mathbf{m}_b \ddot{\mathbf{u}}_b + (\mathbf{c}_b + \mathbf{c}_p) \dot{\mathbf{u}}_b + (\mathbf{k}_b + \mathbf{k}_p) \mathbf{u}_b = -\mathbf{m}_b \mathbf{v}_b \ddot{u}_g(t) + \mathbf{k}_p \mathbf{u}_{sg} \tag{3}$$

\mathbf{m}_b and \mathbf{k}_b are the mass and stiffness matrices of the adjacent buildings, respectively, given by

$$\mathbf{m}_b = \begin{bmatrix} \mathbf{m}_{ln} & 0 \\ 0 & \mathbf{m}_{rm} \end{bmatrix}_{(n+m) \times (n+m)} \tag{4a}$$

$$\mathbf{k}_b = \begin{bmatrix} \mathbf{k}_{ln} & 0 \\ 0 & \mathbf{k}_{rm} \end{bmatrix}_{(n+m) \times (n+m)} \tag{4b}$$

where

$$\mathbf{m}_{ln} = \begin{bmatrix} m_{l1} & 0 & 0 & \dots & 0 & 0 \\ & m_{l2} & 0 & \dots & 0 & 0 \\ & & m_{l3} & \dots & 0 & 0 \\ & & & \ddots & \vdots & \vdots \\ & SYM. & & & m_{l(n-1)} & 0 \\ & & & & & m_{ln} \end{bmatrix}_{n \times n} \tag{5a}$$

$$\mathbf{k}_{ln} = \begin{bmatrix} k_{l1} + k_{l2} & -k_{l2} & 0 & \dots & 0 & 0 \\ & k_{l2} + k_{l3} & -k_{l3} & \dots & 0 & 0 \\ & & k_{l3} + k_{l4} & \dots & 0 & 0 \\ & & & \ddots & \vdots & \vdots \\ & SYM. & & & k_{l(n-1)} + k_{ln} & -k_{ln} \\ & & & & & k_{ln} \end{bmatrix}_{n \times n} \tag{5b}$$

\mathbf{m}_{ln} and \mathbf{k}_{ln} are the mass and stiffness matrices of the n -story left building, respectively, and m_{li} and k_{li} are its mass and stiffness at each story, respectively.

\mathbf{c}_b is the Rayleigh damping matrix of the adjacent buildings which is proportional to the mass and stiffness matrices

$$\mathbf{c}_b = \begin{bmatrix} \mathbf{c}_{ln} & 0 \\ 0 & \mathbf{c}_{rm} \end{bmatrix} = \begin{bmatrix} \alpha_{l0} \mathbf{I}_n & 0 \\ 0 & \alpha_{r0} \mathbf{I}_m \end{bmatrix} \begin{bmatrix} \mathbf{m}_{ln} & 0 \\ 0 & \mathbf{m}_{rm} \end{bmatrix} + \begin{bmatrix} \alpha_{l1} \mathbf{I}_n & 0 \\ 0 & \alpha_{r1} \mathbf{I}_m \end{bmatrix} \begin{bmatrix} \mathbf{k}_{ln} & 0 \\ 0 & \mathbf{k}_{rm} \end{bmatrix} \quad (6)$$

where \mathbf{I}_n and \mathbf{I}_m are identity matrices of n and m size, respectively. α_{l0} and α_{l1} are the Rayleigh coefficients of the left building which are determined from its damping ratio (ξ_l) and first two modal circular frequencies (ω_{l1} and ω_{l2}) as

$$\alpha_{l0} = \xi_l \frac{2\omega_{l1}\omega_{l2}}{\omega_{l1} + \omega_{l2}} \quad (7a)$$

$$\alpha_{l1} = \xi_l \frac{2}{\omega_{l1} + \omega_{l2}} \quad (7b)$$

The mass and stiffness matrices and the Rayleigh coefficient of the m -story right building are determined in a similar way as the mass and stiffness matrices and the Rayleigh coefficient of the n -story left building. Additionally, it is supposed that the number of the stories of the left building is equal or greater than the number of the stories of the right building ($n \geq m$).

$\ddot{\mathbf{u}}_b$, $\dot{\mathbf{u}}_b$ and \mathbf{u}_b are the acceleration, velocity and displacement vectors of the adjacent buildings, respectively, given by

$$\ddot{\mathbf{u}}_b^T = \{ \ddot{u}_{l1} \dots \ddot{u}_{ln} \quad \ddot{u}_{r1} \dots \ddot{u}_{rm} \}_{(n+m)} \quad (8a)$$

$$\dot{\mathbf{u}}_b^T = \{ \dot{u}_{l1} \dots \dot{u}_{ln} \quad \dot{u}_{r1} \dots \dot{u}_{rm} \}_{(n+m)} \quad (8b)$$

$$\mathbf{u}_b^T = \{ u_{l1} \dots u_{ln} \quad u_{r1} \dots u_{rm} \}_{(n+m)} \quad (8c)$$

\ddot{u}_{li} , \dot{u}_{li} and u_{li} are the acceleration, velocity and displacement of the i th story of the left building, respectively, and \ddot{u}_{ri} , \dot{u}_{ri} and u_{ri} are the acceleration, velocity and displacement of the i th story of the right building, respectively, due to earthquake acceleration ($\ddot{u}_g(t)$).

\mathbf{v}_b is the influence vector of the adjacent buildings given by

$$\mathbf{v}_b^T = \{ 1 \dots 1 \quad 1 \dots 1 \}_{(n+m)} \quad (9)$$

\mathbf{u}_{sg} is the vector of separation gap between the adjacent buildings given by

$$\mathbf{u}_{sg}^T = \{ u_{sg1} \dots u_{sgm} \quad 0 \dots 0 \}_{(n+m)} \quad (10)$$

u_{sgi} is the separation gap between the adjacent buildings at the i th story.

\mathbf{k}_{sg} and \mathbf{c}_{sg} are the stiffness and damping matrices of the pounding forces, respectively, given by

$$\mathbf{k}_p = \begin{bmatrix} \mathbf{k}_{sg} & 0 & -\mathbf{k}_{sg} \\ 0 & 0 & 0 \\ -\mathbf{k}_{sg} & 0 & \mathbf{k}_{sg} \end{bmatrix}_{(n+m) \times (n+m)} \quad (11a)$$

$$\mathbf{c}_p = \begin{bmatrix} \mathbf{c}_{sg} & 0 & -\mathbf{c}_{sg} \\ 0 & 0 & 0 \\ -\mathbf{c}_{sg} & 0 & \mathbf{c}_{sg} \end{bmatrix}_{(n+m) \times (n+m)} \quad (11b)$$

where

$$\mathbf{k}_{sg} = \begin{bmatrix} k_{sg1} & \dots & 0 \\ \vdots & \ddots & \vdots \\ 0 & \dots & k_{sgm} \end{bmatrix}_{m \times m} \quad (12a)$$

$$\mathbf{c}_{sg} = \begin{bmatrix} c_{sg1} & \dots & 0 \\ \vdots & \ddots & \vdots \\ 0 & \dots & c_{sgm} \end{bmatrix}_{m \times m} \quad (12b)$$

k_{sg_i} and c_{sg_i} are the pounding stiffness and damping at the i th story, respectively (will be discussed in Section 3). The stiffness and damping matrices of the pounding forces (\mathbf{k}_{sg} and \mathbf{c}_{sg}) provided here are for the case when the all adjacent stories are pounded together. Anyhow, all stories do not necessarily pound together at the same time. The pounding between the adjacent buildings is more likely to occur at the top story of the shorter building and the corresponding story of the adjacent building. Subsequently, lower stories are subjected to the pounding one by one during the earthquake excitation. The pounding forces are only developed at the pounded stories so the possibility of pounding should be checked to determine which stories are pounded together. The components of the stiffness and damping matrices of the pounding forces should be arranged to comply with the developed pounding forces. The possibility of pounding between two adjacent stories is defined by the following boundary condition

$$\delta u_i = u_{li} - (u_{ri} + u_{sg_i}) < 0 \quad \text{no-pounding} \quad (13a)$$

$$\delta u_i = u_{li} - (u_{ri} + u_{sg_i}) \geq 0 \quad \text{pounding} \quad (13b)$$

While the adjacent buildings are vibrating individually and freely (no-pounding condition) the stiffness and damping matrices of the pounding forces are equal to zero. Immediately upon the pounding between the adjacent stories (pounding condition), the stiffness and damping matrices of the pounding forces are developed at the pounded adjacent stories. The stiffness and damping matrices are changed based on the adjacent stories that satisfy the Eq. (13b).

2.2 Solution of the equation

To obtain seismic responses of the adjacent buildings during the earthquake excitation in no-pounding and pounding conditions, a second order linear ordinary differential equation (Eq. (1)) must be solved. However, two different conditions in this equation conceptually mean that it is a nonlinear equation though it is algebraically linear. Step by step procedure is a general solution which is well-suited to solve this type of equation. Newmark (1959) linear acceleration method is a simple, accurate and computationally efficient step by step method, so is employed in this present study.

Newmark linear acceleration method is stable if the time step (Δt) is less than almost half of the fundamental period of the system (T_{rm})

$$\Delta t \leq 0.551 T_{rm} \quad (14)$$

For the two adjacent buildings, fundamental period of the stiffer building (usually the shorter building) is obviously the shortest fundamental period regardless of the pounding and no-pounding conditions, because the fundamental period of the pounded adjacent buildings falls between the fundamental periods of the individual buildings ($T_{ln} > T_p > T_{rm}$). Eq. (14) is never an issue for the seismic analysis of the buildings because relatively smaller time step is chosen to obtain accurate results (time steps equal to or less than 0.01 sec). Indeed, the time steps should be much smaller in the pounding condition than the no-pounding condition due to the high sensitivity of the seismic responses to the time step during pounding condition:

- Pounding duration is maximum $0.5T_p$ because the pounding gives either half sine or truncated half sine response for a complete or weak pounding, respectively (This will be confirmed in section 4.1). First half sine of the response which is compression phase is imaginable while the second half sine which is tension phase is meaningless (i.e., the adjacent buildings push each other but they do not pull each other). Therefore, pounding duration is maximum $0.5T_p$ and the time step must be much smaller than $0.5T_p$ in the pounding condition.
- Rate of the change of the velocity and acceleration of the two subsequent steps is great in the pounding condition and round off errors become very significant. Therefore, very small time steps should be chosen in the time of transferring from pounding to no-pounding conditions and vice versa in order to have accurate results.

This is while very small time steps cost high computational effort and are very time consuming. Therefore, using two different time steps during the analysis could be an efficient idea. Using of time step equal to 0.01 (sec) during no-pounding condition and smaller time steps during pounding condition is proposed in this study. The latter time step is selected based on the following procedure.

Consider a typical SDOF building with mass, lateral stiffness and pounding stiffness equal to 3.0×10^4 kg, 8.89×10^6 N/m and 4.17×10^9 N/m, respectively, subjected to a sinusoidal acceleration. Response of the building is calculated with different time steps. The response of the building corresponding to the smallest time step (0.00001 sec) is considered as the base response and the responses obtained from various time steps are compared to this base response. Response error (i.e., deviation percentage of different responses from the base response) are calculated and shown in Fig. 2 in terms of displacement error and pounding force error. Fluctuation of the response error is observed for the larger time step where the responses are unstable and vary significantly by

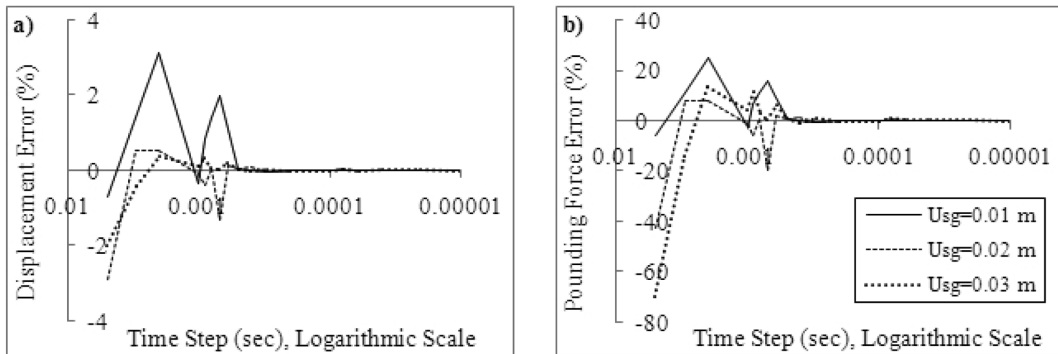


Fig. 2 Response error of the SDOF building subjected to the pounding against the time step

changing the time step. However, the responses tend to become stable and to converge a unique value with negligible errors when the time steps are decreased. Therefore, it is recommended that the time step satisfying the following condition be used for the analyses during the pounding condition (efficiency of this time step is also approved during the numerical study)

$$\Delta t < 0.025 T_{min} \quad (15)$$

T_{min} is fundamental period of the stiffer system (usually the shorter building). For the seismic analysis of the adjacent buildings subjected to earthquake induced pounding, the time step equal to 0.001 sec is found satisfactory and efficient.

Finally the formulation and solution are implemented via a computer program code to carry out the analyses. The computer program code starts with the first step and computes the seismic response with the time step equal to 0.01 sec. Meanwhile the boundary condition (Eq. (13)) is checked to detect the pounding condition. If the no-pounding condition (Eq. (13a)) is satisfied, the computer program code continues until the last second of excitation, though the computer program code stops and goes back to the immediate previous step (i.e., one step before the pounding condition) once the pounding condition (Eq. (13b)) is satisfied. It again re-computes the seismic response for the one step before the pounding condition with the time step equal to 0.001 sec and continues the computation during the pounding. Immediately upon the separation of the buildings, the computer program code continues to the next step (i.e., one step after pounding condition) with the time step equal to 0.001 sec. After this step, the analysis is performed with the time step equal to 0.01 sec. This cycle is repeated during each pounding detected during the analysis until the last second of excitation. This procedure guaranties the computational efficiency with the minimum computation time and optimum storage capacity of the output results.

3. Characteristics of the Kelvin model

Characteristics of the Kelvin model should be determined in order to generate the pounding matrices. Finding the value of its stiffness (pounding stiffness) is an issue which is to be elaborated and solved in the following. Also, the value of its damping (pounding damping) is elaborated and determined in the following.

3.1 Pounding stiffness

In a mass, damping and stiffness system the basic assumption is that the whole mass of the system is concentrated at the center of mass of the story and the all responses (displacement, velocity, acceleration and force) are corresponded to this point (Fig. 3). Regarding to the definition of the separation gap, the distance between the edge of the building and edge of the adjacent structure, an additional virtual distance can be imagined between the center of mass and edge of the building which can be seen in Fig. 3 as u_v . This virtual displacement allows the building to move even further than the separation gap mathematically which means that the building penetrates the adjacent structure ($u_b - u_{sg} > 0$). This penetration is schematically demonstrated in Fig. 3(c) (it will be shown computationally in Fig. 5(a)). Anyhow, this penetration is governed by the equation of motion of the pounded building with the stiffness equal to sum of the pounding stiffness and lateral stiffness of the building.

The Pounding stiffness is best determined by the experiment where it is obtained based on the pounding force recorded during the tests. In the lack of experimental tests, both pounding stiffness and pounding force are unknown, so finding their values demands an iterative procedure. The procedure includes taking a trial value for the pounding stiffness (k_{sgt}) and calculating the pounding force (F_p). To check the convergence of the procedure, the pounding force (F_p) is to be compared with impulsive force (F_{pm}) because the nature of both forces is the same.

According to the Newton's second law of motion, if a force (F_{pm}) acts on a body of mass m , the rate of change of momentum of the body is equal to the applied force, that is

$$\frac{d}{dt}(m\dot{u}) = F_{pm} \quad (16)$$

The mass is constant so the change of momentum is equal to the difference between the initial velocity of contact and the velocity at maximum response. The difference of the velocity is equal to the initial velocity of contact since velocity at maximum response is zero for elastic impact (i.e., the system is fully stopped). Thus, the equation is become

$$F_{pm} = \frac{m_b \dot{u}_{b0}}{\Delta t_F} \quad (17)$$

m_b is the mass of building, \dot{u}_{b0} is the velocity of the building at the beginning of the pounding and

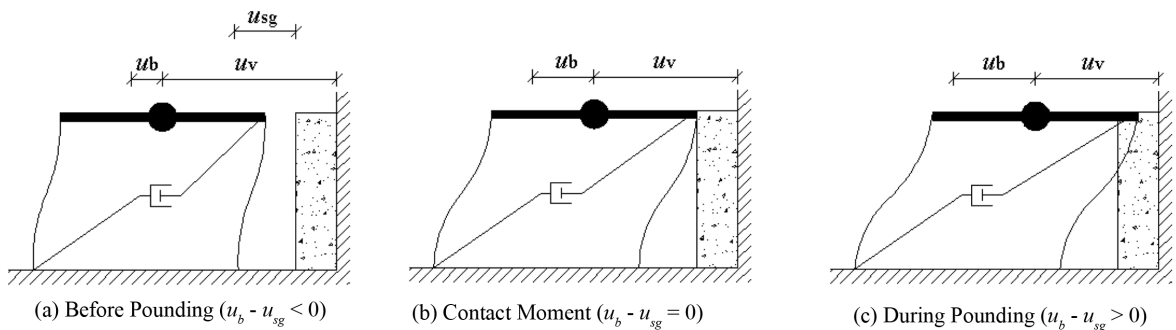


Fig. 3 Schematic response of the SDOF building subjected to the pounding

Δt_F is half time of pounding duration which is obtained from the computation.

The F_p is obtained from Eq. (1) with the trial pounding stiffness. Meanwhile, the velocity of the building at the beginning of the pounding (\dot{u}_{b0}) and the half time of pounding duration (Δt_F) are obtained. By \dot{u}_{b0} and Δt_F are obtained, the F_{pm} is calculated from Eq. (17). If the values of F_p and F_{pm} are equal, the corresponding trial pounding stiffness is the real value of the pounding stiffness. It is reasonable to take the lateral stiffness of the building as an initial value for the trial pounding stiffness. Because the pounding stiffness is several times the lateral stiffness of the building, the trial pounding stiffness should be increased and the procedure should be repeated until the convergence.

Pounding of a free vibrating SDOF building due to an initial displacement of 0.1 m is considered here to validate the proposed procedure of finding of the pounding stiffness. Three previous studies on building pounding are selected; experimental studies by Chau *et al.* (2003) and Filiatrault *et al.* (1995) and numerical study by Maison and Kasai (1990). The characteristics of the pounding building are taken from these papers and the real values of the pounding stiffnesses are calculated via the proposal procedure.

Normalization of calculated pounding force (F_p) with impulsive force (F_{pm}) and showing the normalized pounding force (F_{pm}/F_p) with respect to the corresponding normalized pounding stiffness (k_{sgt}/k_{sge}) (k_{sgt} is the trial pounding stiffness and k_{sge} is the real pounding stiffness taken from previous researches) leads to graph like Fig. 4. In the early stage of the graph where the trial pounding stiffness is relatively small, normalized pounding force grows up with increment of the normalized pounding stiffness. Where the normalized pounding stiffness is about one, the normalized pounding force is around one, too. From this stage onward, the normalized pounding force keeps constant and equal to one with increment of the normalized pounding stiffness. This means that the normalized pounding force is converged and F_p is equal to F_{pm} . This implies that the real value of the pounding stiffness obtained from the proposal procedure approximates very well the real value of the pounding stiffness taken from experiment because the unit value of the normalized pounding force is taken place about the unit value of the normalized pounding stiffness. Consequently, the proposal procedure of finding the pounding stiffness sounds very good method in the lack of experimental results. According to our analyses the pounding stiffness could be best described by the lateral stiffness of the building which is in the range of 50 to 100 times the lateral stiffness of the building.

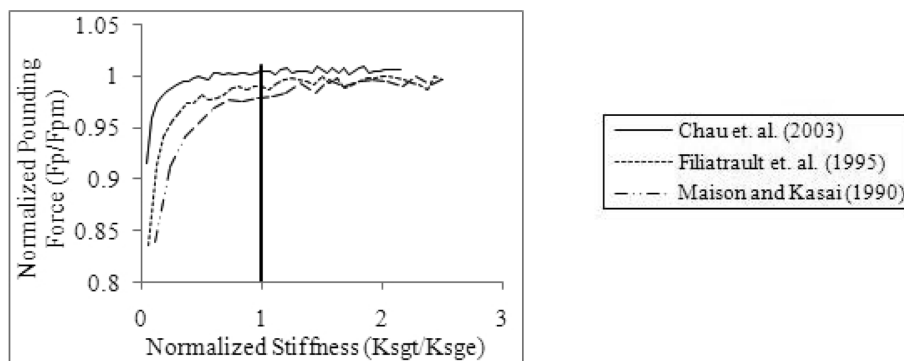


Fig. 4 The normalized pounding force against the normalized stiffness

3.2 Pounding damping

Damping coefficient is representation of energy dissipation during the pounding which is obtained from

$$c_{sgi} = 2\xi \sqrt{k_{sgi} \frac{m_{li}m_{ri}}{m_{li} + m_{ri}}} \quad (18)$$

where

$$\xi = -\frac{lne}{\sqrt{\pi^2 + lne^2}} \quad (19)$$

e is the coefficient of restitution which is the ratio of the contact and separation velocities (i.e., start and end velocities) of the impact.

$$e = \frac{(\dot{u}_{li} - \dot{u}_{ri})_{start}}{(\dot{u}_{li} - \dot{u}_{ri})_{end}} \quad (20)$$

Coefficient of restitution (e) ranges between 0 and 1 for pure plastic and elastic impacts, respectively. Laboratory tests conducted by Jankowski (2009) in order to evaluate the interactions between elements made of different building materials during the pounding indicates that the coefficient of restitution highly depends on both contact velocity and material used. Lower coefficient of restitutions for higher contact velocities exhibits that significant plastic deformations and energy dissipations are anticipated for higher contact velocities. Jankowski (2009) suggests the using of different coefficient of restitutions according to the contact velocities during the time history analysis for more accuracy. However, due to lack of appropriate data, it should be more investigated and use of one coefficient of restitution for the all poundings is acceptable at the moment.

Typical values of the coefficient of restitution in various applications for metals are between 1.00 and 0.60 (Nguyen *et al.* 1986). Rajalingham and Rakheja (2000) state that the coefficient of restitutions less than unity and greater than 0.49 ($0.49 < e < 1.00$) are acceptable in decreasing the pounding force while values less than $e < 0.30$ are undesirable in constructive engineering applications. Anagnostopoulos and Spiliopoulos (1992) and Maison and Kasai (1992) recommend intervals of $0.50 < e < 0.75$ and $0.53 < e < 0.85$, respectively, for typical buildings, although smaller value ($e = 0.40$) has been used by Zhu *et al.* (2002). While the practical range of the coefficient of restitution has been determined by previous researchers, they generally believed that various coefficient of restitution had less and even negligible influence in overall response of the building. Jankowski (2008), Anagnostopoulos (1988) have chosen the value of $e = 0.65$ which seems a reasonable value of coefficient of restitution in practical building analyses which is used in this study.

4. Numerical study

Initially, free vibration of a SDOF building with both linear elastic and visco-elastic behaviors pounded to an adjacent rigid structure is presented (the linear elastic case was treated by Maison and Kasai (1990)). Then, an example of pounding between two multistory adjacent buildings due to

earthquake excitation (MDOF pounding case) is given and effects of separation gap, buildings height and earthquake excitations are investigated.

4.1 SDOF pounding case

The SDOF building vibrates freely due to an initial displacement of 0.021 m, however, it pounds to the adjacent structure if it is located 0.01 m from the rigid structure. The SDOF building consists of mass (17.6 kg), stiffness (544 N/m), damping ratio ($\xi = 0.02$), pounding stiffness (22660 N/m) and coefficient of restitution ($e = 0.65$). The period of building is $T_b = 1.13$ sec and $T_p = 0.17$ sec for no-pounding and pounding conditions, respectively. Equation of motion of pounding of this SDOF building is derived from Eq. (1) where there is only left one story building

$$m_1 \ddot{u}_1 + (c_1 + c_p) \dot{u}_1 + (k_1 + k_p) u_1 = k_p u_{sg} \quad (21)$$

Time histories of the displacement, velocity and acceleration corresponding to the first cycle of vibration are shown in Fig. 5. In addition, relationship between displacement and velocity is shown in Fig. 6 in phase plane.

Fig. 5(a) shows time history of the displacement of this SDOF building. In the no-pounding case, the maximum displacements of elastic and visco-elastic buildings are equal to 0.020 m and 0.019 m, respectively. In the pounding case, the separation gap of 0.01 m prevents the building to reach its maximum displacement. The building moves toward the rigid structure until the pounding occurs at

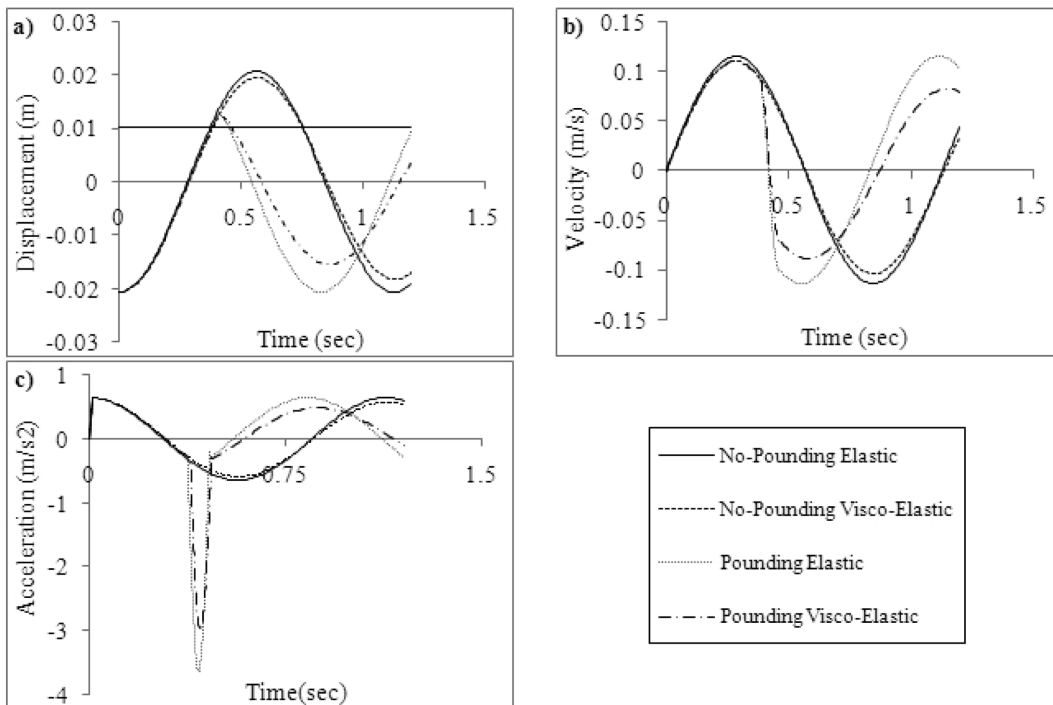


Fig. 5 Response of the SDOF building subjected to the pounding; (a) displacement, (b) velocity, (c) acceleration

the displacement of 0.01 m. The visco-elastic building pounds to the rigid structure 0.01 sec later than the elastic building while this time lag is due to energy dissipation during the vibration which reduces the amplitude of displacement. In the first half time of the pounding the building still tends to move toward the rigid structure beyond the separation gap ($u_b > u_{sg} = 0.010$ m) meaning that the building penetrates the rigid structure as it is shown schematically in Fig. 3. On the other hand, the rigid structure resists against the building and stops it at the maximum penetration of 0.003 m and 0.002 m for the elastic and visco-elastic poundings, respectively. The rigid structure pushes the building away until the building separates from the rigid structure. The duration of pounding (penetration) is 0.084 sec which is half time of the period of the building in pounding condition ($T_p = 0.17$ sec). In the pounding case, the building becomes stiffer due to additional pounding stiffness and its maximum displacements are 0.013 m and 0.012 m for the elastic and visco-elastic buildings, respectively. Consequently, the maximum displacement in the pounding case is less than the no-pounding case and the reduction depends on the separation gap and characteristics of the contact force model.

Fig. 5(b) shows time history of the velocity of the SDOF building. The velocity is initially zero but is increased continuously until the pounding. When the pounding occurs the rigid structure prevents further movement of the building and causes a sharp reduction in the velocity of the building. Reduction of the velocity is perfectly consistent with the displacement of the building during the pounding. The velocity is first derivation of the displacement with respect to the time ($\dot{u}_b = du_b/dt$) so it has $\pi/2$ phase difference with the displacement (Fig. 6). The displacement and velocity follow each other in a circle and a spiral routes in the elastic and visco-elastic buildings. This allows the velocity to be decreased dramatically and to reach to zero value exactly at the time with the maximum displacement during the pounding meaning that the building is stopped. Sign of velocity is changed from positive to negative meaning that the building moves in the opposite direction to the approaching direction. The absolute velocity is increased rapidly in negative state until the building separates from the rigid structure. The initial velocities (start velocities) of the pounding are almost the same for both elastic and visco-elastic buildings but the separation velocity (end velocity) of the visco-elastic building is much less than the elastic building. Absolute velocities at the start and end of pounding in elastic building are exactly the same ($|\dot{u}_b| = 0.10$ m/s) whereas in the visco-elastic building, the start velocity ($|\dot{u}_b| = 0.09$ m/s) and end velocity ($|\dot{u}_b| = 0.07$ m/s) differ obviously. In the latter case, the difference between the start and end velocities during the pounding

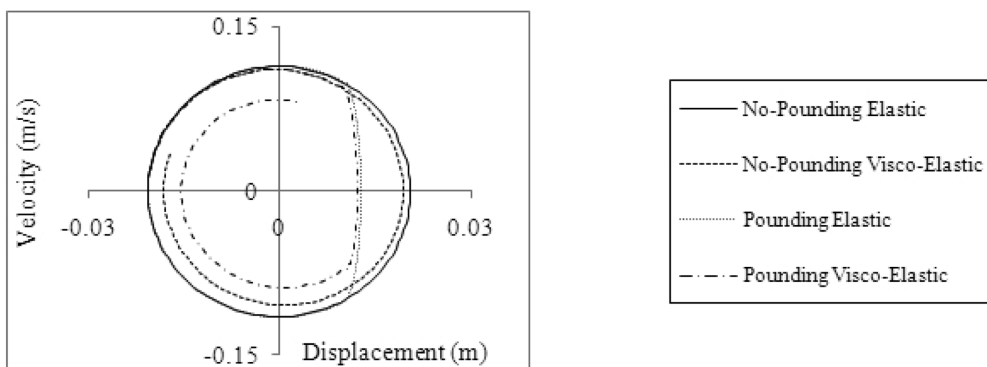


Fig. 6 Response of the SDOF building subjected to the pounding in phase plane

correlates to the energy dissipation and depends on the coefficient of restitution and therefore material properties.

Fig. 5(c) shows time history of the acceleration of the SDOF building. The acceleration of the building starts from $\ddot{u}_0 = 0.64 \text{ m/s}^2$ due to initial displacement of $u_{b0} = -0.02 \text{ m}$ and is decreased initially. The acceleration is the first derivation of the velocity and the second derivation of the displacement with respect to the time ($\ddot{u}_b = d\dot{u}_b/dt = d^2u_b/dt^2$) thus it has π phase difference with the displacement. Immediately upon the pounding, the acceleration is -0.32 m/s^2 but it falls down drastically during the first half time of the pounding. Descending of the acceleration is due to rapid reduction of the velocity. Then the acceleration is increased sharply due to absolute increment of the velocity. For the elastic pounding, the maximum absolute value of acceleration (3.63 m/s^2) occurs at zero velocity and the maximum displacement during pounding. For the visco-elastic pounding, similar to the elastic pounding, the acceleration is decreased rapidly due to pounding and then increased sharply, but, the maximum absolute value of acceleration (2.98 m/s^2) is lower for the visco-elastic pounding because of dissipation of energy during the pounding.

Fig. 7(a) shows time history of the pounding force of the SDOF building. Immediately upon the pounding, the pounding force is produced and increased rapidly. It acts opposite to the movement direction, prevents further movement of the building and pushes the building away from rigid structure. The pounding force is correlated to the displacement and velocity of the building (Eq. (2)). When the building is pounded, large pounding force is produced as the acceleration is increased. Lets the origin of the displacement is shifted to the separation gap so the discussion is concentrated on the responses during the pounding only. For the elastic building, the pounding force is proportional to only the displacement. When the pounding occurs, at the beginning of the pounding the displacement is zero so the pounding force is zero. The pounding force is increased with the displacement increment (penetration). The pounding force reaches to its maximum value equal to 55.01 N at the time when the displacement is maximum (maximum penetration). Then the pounding force is decreased with the displacement reduction and becomes zero at the separation instant. Rate of increment and rate of reduction of the pounding force is exactly the same in the elastic pounding which produces a linear relationship between the pounding force and displacement as shown in Fig. 7(b). On the other hand, the pounding force of visco-elastic pounding is proportional to both displacement and velocity. At the beginning of the pounding, the displacement is zero while the velocity is a positive value which produces the pounding force equal to 11.26 N . The maximum value of pounding force is 45.07 N for the visco-elastic pounding which is less than

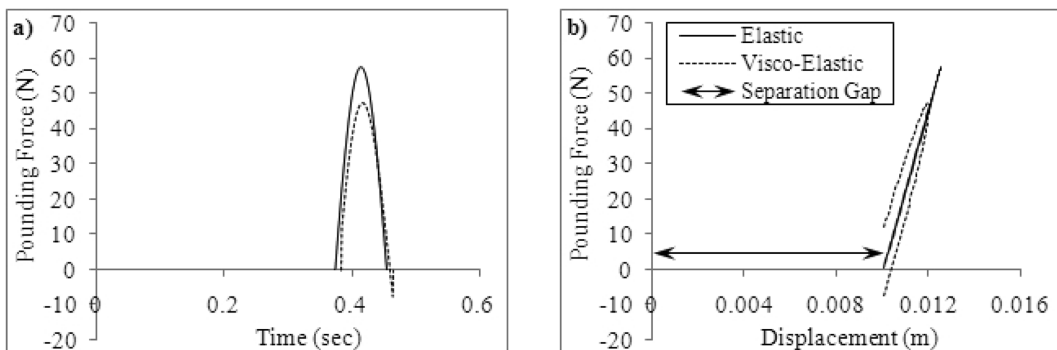


Fig. 7 The pounding force developed during the pounding and its relationship with displacement

the elastic pounding because some energy dissipates during the visco-elastic pounding. The pounding force is decreased with the displacement reduction, however, it is not zero at the separation instant. At the end of pounding, the displacement is zero but the separation velocity is a negative value which has opposite sign comparing to the contact velocity, meaning that the negative pounding force or pulling force equal to -7.24 N is produced. This force does not have any physical meaning because the masses push each other only, so this unnoticeable pulling force must be ignored. The rate of increment and rate of reduction of the pounding force are different in the visco-elastic pounding, producing a relationship between the pounding force and displacement as shown in Fig. 7(b).

4.2 Pounding between the multistory adjacent buildings

Seismic responses of adjacent buildings subjected to earthquake induced pounding are investigated. Building configuration comprises a steel building (ST building) placed at the left side and a reinforced concrete building (RC building) placed at the right side. All buildings are supposed to be residential buildings with mass of 100 Tons per story. Energy dissipation is higher in the RC building than the ST building where corresponding damping ratios are 0.05 and 0.02, respectively. For each building, the lateral stiffness is constant for all stories and it is chosen in a way that gives fundamental period of the building (T_{ST} , T_{RC}) in compliance with the fundamental period recommended by ASCE (2006) as

$$T_{ST} = 0.0724(H)^{0.8} \quad (22a)$$

$$T_{RC} = 0.0466(H)^{0.9} \quad (22b)$$

where H is the building height. The pounding stiffness is equal to 1.0×10^{10} N/m and the coefficient of restitution is equal to 0.65. To evaluate the seismic response of adjacent buildings for different conditions, acceleration of the earthquake excitation is applied to the buildings' base.

A case of pounding between a 8-story ST building (8-ST) adjacent to a 4-story RC building (4-RC) subjected to the El Centro earthquake is presented here. Figs. 8-11 show envelopes of the maximum seismic responses (i.e., displacement, story drift, story shear and overturning moment (OTM)) of adjacent buildings without and with pounding. The displacement of 8-ST building is

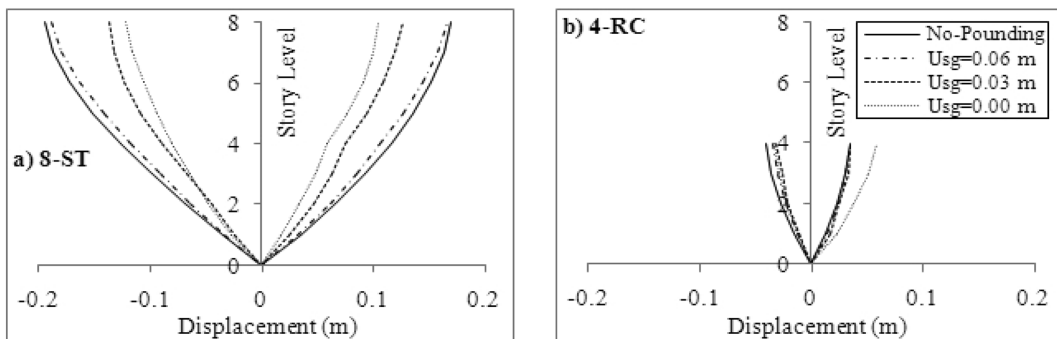


Fig. 8 Envelopes of the maximum displacements of the adjacent buildings

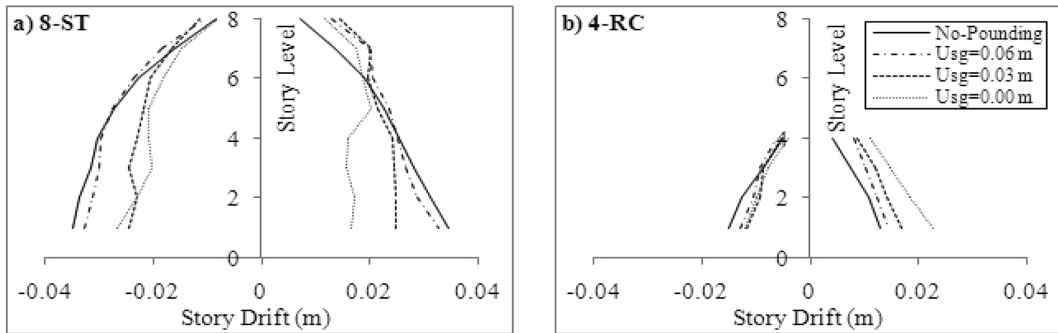


Fig. 9 Envelopes of the maximum story drifts of the adjacent buildings

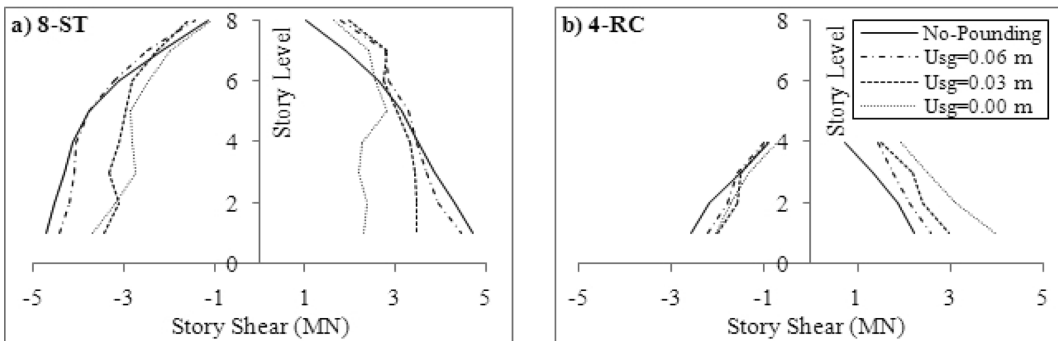


Fig. 10 Envelopes of the maximum story shears of the adjacent buildings

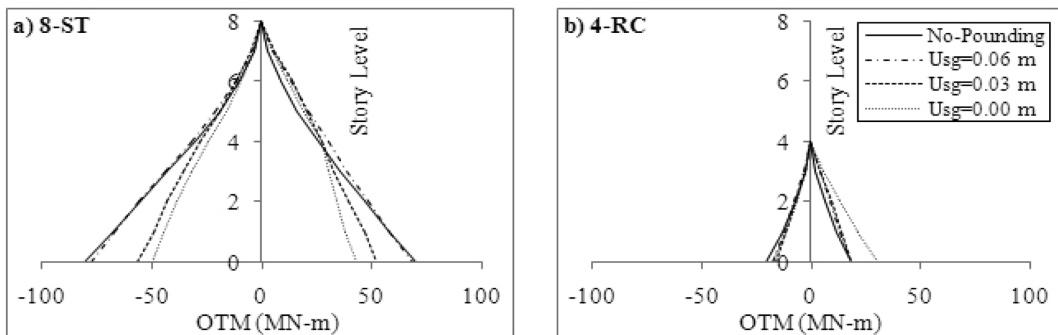


Fig. 11 Envelopes of the maximum OTMs of the adjacent buildings

reduced when pounding occurs and the reduction is highlighted when the separation gap is smaller (Fig. 8(a)). The story drifts of 8-ST building are decreased for the lower stories while increased for the upper stories (Fig. 9(a)). A sudden change of displacement and story drift is observed in the graphs of pounding cases. The critical change of the story shear and OTM are observed in the upper stories of 8-ST building where they are increased due to the increment of story drift as shown in Figs. 10(a) and 11(a), respectively. The seismic responses of 4-RC building are decreased in pounding side whereas increased in no-pounding side. The critical change of seismic responses of

4-RC building due to pounding is increment of the displacement, story drift, story shear and OTM in no-pounding side, as shown in Figs. 8(a)-11(a), respectively.

Time histories of the displacements of 4th story of adjacent buildings are shown in Fig. 12. When the adjacent buildings do not pound together (Fig. 12(a)), forms of the displacements are different and the amplitude of displacement of 8-ST building is higher than 4-RC building. When they pound together (Fig. 12(b)), they interact together and displacement of each building is affected by the other building. The 4-RC building resists against movement of 8-ST building and reduces its displacement amplitude. Meanwhile, the 8-ST building withstands against the movement of 4-RC building and pushes it away and increases its displacement amplitude.

To sum up, the pounding impacts both buildings negatively. The critical condition is occurred due to pounding where the seismic responses are increased. Although the displacement of 8-ST building is reduced but the story drift, story shear and OTM are increased, particularly in the upper stories in pounding side. For the 4-RC building, the displacement, story drift, story shears and OTM are all increased in no-pounding side. The most critical condition is occurred at the top story of each building.

4.3 Effect of the separation gap

The separation gap between the adjacent buildings plays the key role in earthquake induced pounding. The configuration of the 8-ST building adjacent to the 4-RC building is considered here while the buildings are subjected to the pounding due to the El Centro earthquake. The analyses are

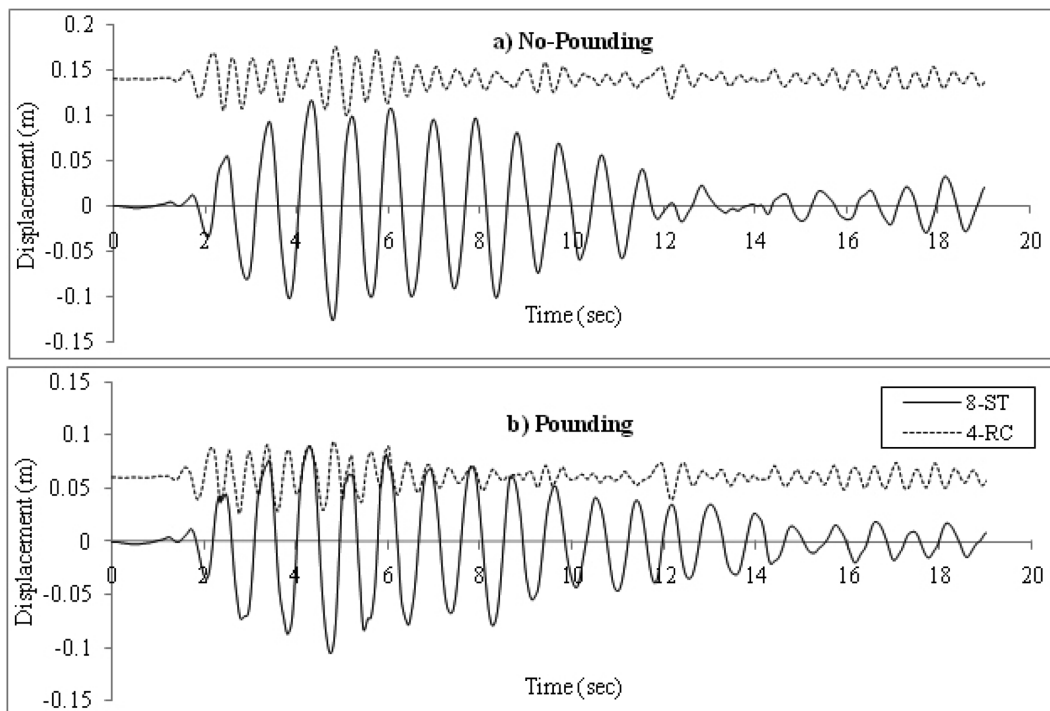


Fig. 12 Time history of the displacements of the 4th story of adjacent buildings due to the El Centro earthquake; a) no-pounding, b) pounding with separation gap of 0.06 m

repeated for varying separation gaps. Variations of the maximum displacements and story shears of the buildings for different separation gap ratios are shown in Figs. 13 and 14, respectively. The separation gap ratio is the ratio of the separation gap of a particular building configuration to the minimum separation gap required to prevent pounding (0.13 m).

The smaller the separation gap ratio the smaller the displacement for the 8-ST building whereas the larger the displacement for the 4-RC building (Fig. 13). At zero separation gap, the displacement is decreased around 40% for the 8-ST building while increased almost 70% for the 4-RC building due to the pounding. The story shears of both buildings are increased due to pounding with reduction of separation gap ratio (Fig. 14). Particularly for the top stories, these increments are up to 117% and 174% for the 8-ST building and the 4-RC building, respectively. Slight jumps are also observed in these figures that are due to contribution of different stories in the pounding. All the stories contribute in the pounding if the separation gap is small. The lower stories are eliminated one by one with increment of the separation gap. Finally, for relatively large separation gaps the 4th stories pound together only. The pounding force is produced at the stories that are pounded together as shown in Fig. 15.

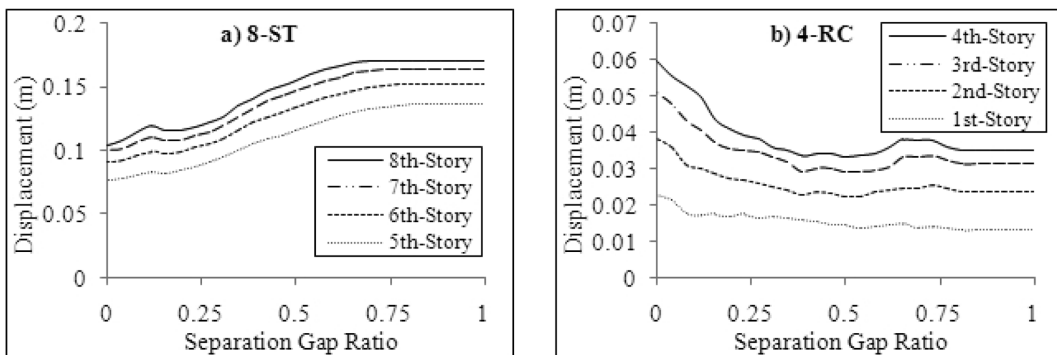


Fig. 13 Relationship between the variation of the maximum displacements of the adjacent buildings and the separation gap ratio

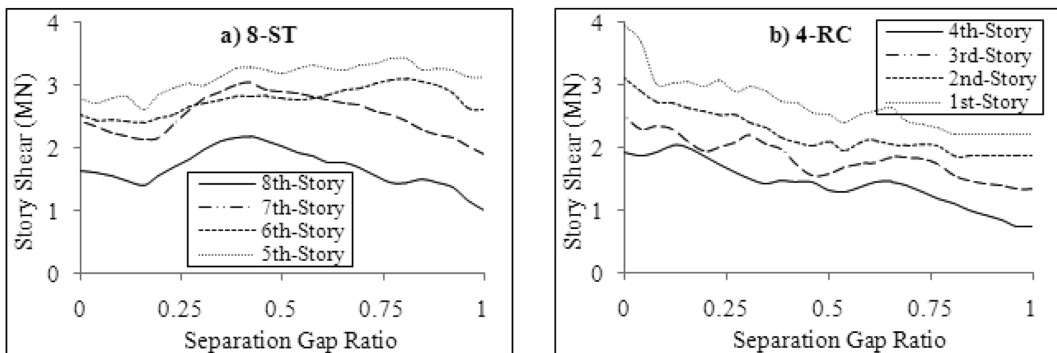


Fig. 14 Relationship between the variation of the maximum story shears of the adjacent buildings and the separation gap ratio

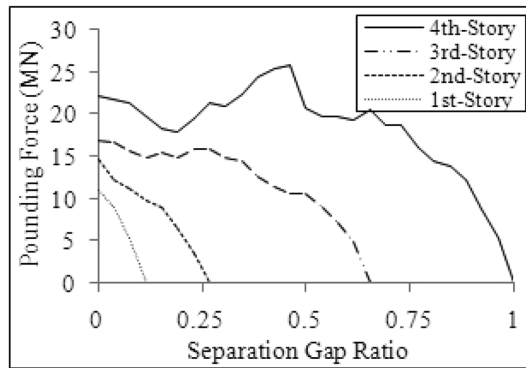


Fig. 15 Relationship between the variation of the produced pounding force with the separation gap ratio

4.4 Effect of the building height

The pounding is more likely to occur if the adjacent buildings are vibrating out of phase. Two of the factors that cause the adjacent buildings vibrate out of phase are different building height and material. To have the buildings of varying heights, the number of stories of ST building (the left and taller building) is 6, 8 or 10 for different building configurations and the number of stories of RC building (the right and shorter building) is equal or less than the number of stories of ST building in its configuration. The building configuration is out of phase when the period ratio (T_{ST}/T_{RC}) is nearer to 0.2 and it is in-phase when the period ratio is nearer to 0.8. In the out of phase building configurations the RC building is very short and has 2 or 3 stories while in the in-phase building configurations the RC building is relatively tall with 1 or 2 stories less than the ST building.

Figs. 16 and 17 shows variations of the displacement and story shear ratios of the top stories of ST and RC buildings subjected to the El Centro earthquake with respect to the period ratio (displacement/story shear ratio is the ratio of the maximum displacement/story shear of building in pounding condition to the maximum displacement/story shear of building in no-pounding condition.). The displacement ratios are less than one for the ST building because its displacements are reduced when the pounding occurs (down to 0.56 times), however, the reduction is not very important when the building configuration is very out of phase (Fig. 16(a)). It implies that very short RC buildings do not affect the tall ST buildings seriously. On the other hand, the displacement ratios are more than one for the RC building because its displacements are increased significantly due to the pounding (up to 3.78 times) and the increments are very serious when the building configuration is out of phase (Fig. 16(b)). In very out of phase building configurations, the tall ST building shares the major mass of building configuration during the pounding and governs the movement of both buildings. While the short RC building shares the minor mass of building configuration during the pounding and is completely affected by the tall ST building. The story shears are greater than one for both buildings and all period ratios (Fig. 17) because the story shears of the top stories of both buildings are increased due to the pounding (up to 2.25 times for the tall ST building and 4.64 times for the short RC building). The increment is similar for both tall ST and short RC buildings when the building configuration is almost in-phase. When the building configuration is almost out of phase, the increment of story shear is small in the tall ST building though it is substantial in the short RC building. Consequently, the short RC building suffers more

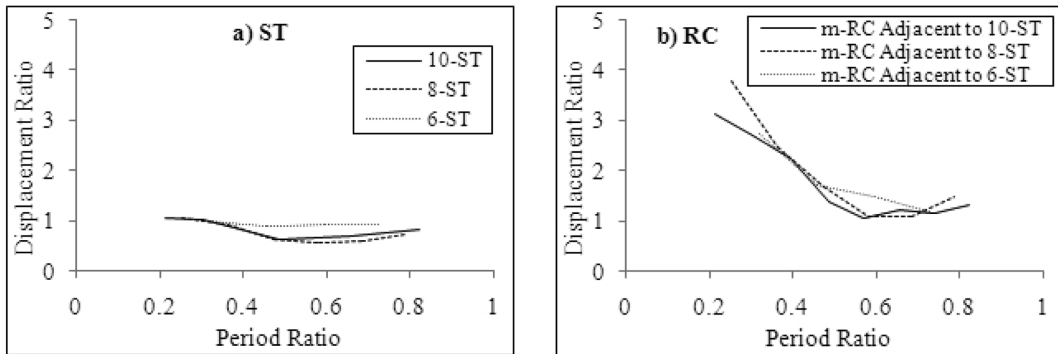


Fig. 16 Relationship between the variation of the maximum displacement in the top stories of adjacent buildings and the period ratio

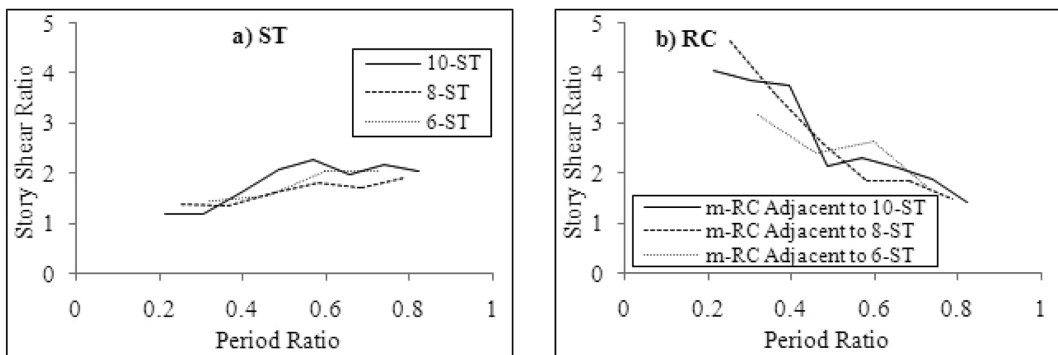


Fig. 17 Relationship between the variation of the maximum story shear in the top stories of adjacent buildings and the period ratio

seriously from the pounding than the tall ST building particularly if the heights of buildings are significantly different.

4.5 Effect of the earthquake excitation

Earthquake excitation is one of the major sources of the building movement and probable pounding between the adjacent buildings. The building movement and probable pounding between the adjacent buildings are affected by the earthquake excitation depending on the fundamental period/frequency of the building and dominant period/frequency of the earthquake excitations. Characteristics of the earthquake excitations including their dominant frequencies are presented in Table 1. The configuration of the 8-ST building adjacent to the 4-RC building is considered here while the fundamental period of the 8-ST building is 0.92 sec (fundamental frequency 1.09 Hz) and the fundamental period of the 4-RC building is 0.44 sec (fundamental frequency 2.27 Hz). If the adjacent buildings are pounded together in the all stories, the fundamental period of pounded building configuration is 0.74 sec (fundamental frequency 1.35 Hz).

The seismic responses of adjacent buildings due to different earthquake excitations are computed

Table 1 Characteristics of the earthquake excitations

| Earthquake | Year | Record/Component | Magnitude | PGA (g) | Dominant Frequency (Hz) |
|---------------------|------|-------------------|-----------|---------|-------------------------|
| San Fernando | 1971 | SFERN/ORR021 | 6.6 | 0.32 | 2.94 |
| Loma Prieta | 1989 | LOMAP/G01090 | 6.9 | 0.47 | 2.70 |
| Superstitt Hills(B) | 1987 | SUPERST/B-SUP045 | 6.7 | 0.68 | 2.04 |
| Victoria, Mexico | 1980 | VICT/CPE045 | - | 0.62 | 1.75 |
| El-Centro | 1940 | IMPVALL/I-ELC180 | 7 | 0.31 | 1.47 |
| Westmorland | 1981 | WESTMORL/WSM180 | 5.8 | 0.50 | 1.41 |
| Livermore | 1980 | LIVERMOR/B-KOD180 | 5.4 | 0.30 | 1.32 |
| Kocaeli, Turkey | 1999 | KOCAELI/ATS000 | 7.4 | 0.25 | 1.12 |
| Landers | 1992 | LANDERS/YER270 | 7.3 | 0.25 | 0.73 |
| Kobe | 1995 | KOBE/KAK090 | 6.9 | 0.35 | 0.58 |

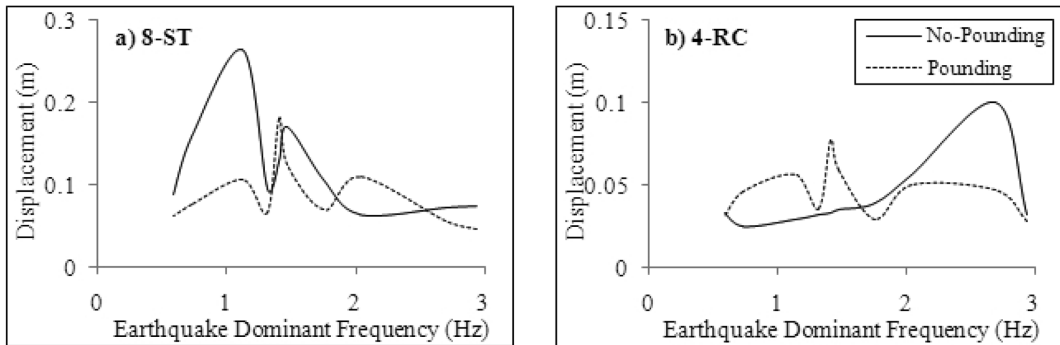


Fig. 18 Relationship between the variation of the maximum displacement in the top stories of adjacent buildings and the earthquake dominant frequency

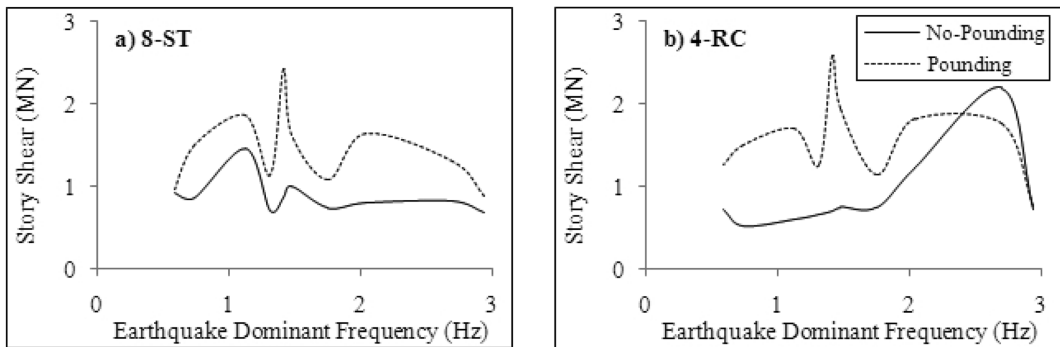


Fig. 19 Relationship between the variation of the maximum story shear in the top stories of adjacent buildings and the earthquake dominant frequency

separately. The maximum displacements and story shears produced at the top stories of adjacent buildings for different earthquakes are shown in Figs. 18 and 19, respectively. When the buildings

are vibrating separately and do not pound together; the maximum displacement (0.26 m, Fig. 18(a)) and story shear (1.46 MN, Fig. 19(a)) of 8-ST building are produced due to the Kokaeli, Turkey earthquake while the maximum displacement (0.10 m, Fig. 18(b)) and story shear (2.18 MN, Fig. 19(b)) of 4-RC building are produced due to the Loma Prieta earthquake. When the buildings are located immediately from each other, they pound together and there is interaction between them. This interaction causes the buildings accompany each other during the vibration and vibrate based on the fundamental period similar to the fundamental period of the pounded building configuration. It is observed from Figs. 18 and 19 that the variations of the displacements and story shears produced at the top stories of both buildings are similar. The maximum displacements and story shears are produced due to the Westmorland earthquake; the maximum displacement is 0.18 m (Fig. 18(a)) and 0.08 m (Fig. 18(b)) for the 8-ST and 4-RC buildings, respectively, and the maximum story shear is 2.42 MN (Fig. 19(a)) and 2.57 MN (Fig. 19(b)) for the 8-ST and 4-RC buildings, respectively.

It is concluded that, in order to have the effect of earthquake induced pounding on the seismic responses of the adjacent buildings, it is vital that the characteristics of the potential earthquake at the site where the buildings are located to be determined initially. Each building configuration possesses three different fundamental periods demonstrating a unique seismic response due to a unique earthquake excitation. Therefore, the effect of earthquake induced pounding on each building configuration must be evaluated case by case knowing that it is detrimental most of the times.

5. Conclusions

The formulations are presented and an efficient solution with optimum time step provided to obtain the seismic responses of the adjacent buildings subjected to earthquake induced pounding. The pounding force is developed by means of the Kelvin contact force model and its characteristics are elaborated and a new iterative procedure is proposed to determine the pounding stiffness. The pounding between adjacent buildings is elaborated and discussed through the numerical and parametric study. The effects of separation gap, building height and earthquake excitation on the pounding between a steel building adjacent to a reinforced concrete building are investigated. The results show that the pounding generally worsens the buildings conditions mostly because of increasing the developed story shears. When the separation gap is smaller the effect of pounding is highlighter and more stories contribute in the pounding. Different height causes the buildings vibrate out of phase and pound together, anyhow, when the different is significant, the taller building is less affected whereas the shorter building is more affected from the pounding. Finally, it is found that the effect of earthquake induced pounding on each building configuration must be evaluated case by case based on the potential earthquake at the area. Each building configuration possesses three different fundamental periods demonstrating a unique seismic response due to a unique earthquake excitation.

References

- Abdel Raheem, S.E. (2006), "Seismic pounding between adjacent building structures", *Electron. J. Struct. Eng.*, **6**, 66-74.

- Anagnostopoulos, S.A. (1988), "Pounding of buildings in series during earthquakes", *Earthq. Eng. Struct. D.*, **16**, 443-456.
- Anagnostopoulos, S.A. and Spiliopoulos, K.V. (1992), "An investigation of earthquake induced pounding between adjacent buildings", *Earthq. Eng. Struct. D.*, **21**, 289-302.
- ASCE (2006), *Minimum Design Loads for Buildings and Other Structures*, American Society of Civil Engineers, SEI 7-05, Alexander Bell Drive, Reston, Virginia.
- Chau, K.T. and Wei, X.X. (2001), "Pounding of structures modelled as non-linear impacts of two oscillators", *Earthq. Eng. Struct. D.*, **30**, 633-651.
- Chau, K.T., Wei, X.X., Guo, X. and Shen, C.Y. (2003), "Experimental and theoretical simulations of seismic poundings between two adjacent structures", *Earthq. Eng. Struct. D.*, **32**, 537-554.
- Chopra, A.K. (2007), *Dynamics of Structures: Theory and Application to Earthquake Engineering*, Prentice Hall, Englewood Cliffs, NJ.
- Cole, G., Dhakal, R., Carr, A. and Bull, D. (2011), "An investigation of the effects of mass distribution on pounding structures", *Earthq. Eng. Struct. D.*, **40**, 641-659.
- Davis, R.O. (1992), "Pounding of buildings modelled by an impact oscillator", *Earthq. Eng. Struct. D.*, **21**, 253-274.
- Favvata, M.J., Karayannis, C.G. and Liolios, A.A. (2009), "Influence of exterior joint effect on the inter-story pounding interaction of structures", *Struct. Eng. Mech.*, **33**(2), 113-136.
- Filiatrault, A., Wagner, P. and Cherry, S. (1995), "Analytical prediction of experimental building pounding", *Earthq. Eng. Struct. D.*, **24**, 1131-1154.
- Goldsmith, W. (1960), *Impact: The Theory and Physical Behaviour of Colliding Solids*, Edward Arnold, London.
- Jankowski, R. (2008), "Earthquake induced pounding between equal height buildings with substantially different dynamic properties", *Eng. Struct.*, **30**, 2818-2829.
- Jankowski, R. (2009), "Experimental study on earthquake-induced pounding between structural elements made of different building materials", *Earthq. Eng. Struct. D.*, **39**(3), 343-354.
- Kim, S.H. and Hon, M.S. (2003), "Effects of seismically induced pounding at expansion joints of concrete bridges", *J. Eng. Mech.*, **129**(11), 1225-1234.
- Mahin, S.A., Bertero, V.V., Chopra, A.K. and Collins, R.G. (1976), *Response of the Olive View hospital main building during the San Fernando earthquake*, Report No. EERC 76-22, Earthquake Engineering Research Center, University of California, Berkeley, CA.
- Mahmoud, S. and Jankowski, R. (2010) "Pounding-involved response of isolated and non-isolated buildings under earthquake excitation", *Earthq. Struct.*, **1**(3), 231-252.
- Maison, B.F. and Kasai, K. (1990), "Analysis for type of structural pounding", *J. Struct. Eng.*, **116**(4), 957-977.
- Maison, B.F. and Kasai, K. (1992), "Dynamics of pounding when two buildings collide", *Earthq. Eng. Struct. D.*, **21**, 771-786.
- Muthukumar, S. and DesRoches, R. (2006), "A Hertz contact model with non-linear damping for pounding simulation", *Earthq. Eng. Struct. D.*, **35**, 811-828.
- Newmark, N.M. (1959), "A method of computation for structural dynamics" *J. Eng. Mech. Div., ASCE*, **85**, 67-94.
- Nguyen, D.T., Noah, S.T. and Kettleborough, C.F. (1986), "Impact behaviour of an oscillator with limiting stops, Part I: a parametric study", *J. Sound Vib.*, **109**(2), 293-307.
- Pantelides, C.P. and Mat, X. (1998), "Linear and non linear pounding of structural systems", *Comput. Struct.*, **66**(1), 79-92.
- Papadrakakis, M. and Mouzakis, H.P. (1995), "Earthquake simulator testing of pounding between buildings", *Earthq. Eng. Struct. D.*, **24**, 811-834.
- Polycarpou, P.C. and Komodromos, P. (2011), "Numerical investigation of potential mitigation measures for poundings of seismically isolated buildings", *Earthq. Struct.*, **2**(1), 1-24.
- Rajalingham, C. and Rakheja, S. (2000), "Analysis of impact force variation during collision of two bodies using a single degree of freedom system model", *J. Sound Vib.*, **229**(4), 823-835.
- Rezavandi, A. and Moghadam, A.S. (2007), "Experimental and numerical study on pounding effects and mitigation techniques for adjacent structures", *Adv. Struct. Eng.*, **10**(2), 121-134.
- Wolf, J.P. and Skrikerud, P.E. (1980), "Mutual pounding of adjacent structures during earthquakes", *Nucl. Eng.*

Des., **57**, 253-275.

Zhu, P., Abe, M. and Fujino, Y. (2002), "Modelling three-dimensional non-linear seismic performance of elevated bridges with emphasis on pounding of girders", *Earthq. Eng. Struct. D.*, **31**, 1891-1913.